*J. Synchrotron Rad.* (1998). **5**, 443–444

# Insertion devices for BESSY II

**J. Bahrdt,* A. Gaupp, G. Ingold, M. Scheer and W. Gudat**

*BESSYmbH, Lentzeallee 100, 14195 Berlin, Germany. E-mail: bahrdt@bessy.de*

(*Received 4 August 1997; accepted 15 October 1997*)

The high-brilliance synchrotron radiation source BESSY II will provide space for the installation of 14 insertion devices. At the time of writing (July 1997), eight insertion devices are funded. The first light for use by scientists will be available in January 1999. The undulators are designed for a scanning operation in parallel with the monochromator. This modus requires tight tolerances concerning the drive system. The first insertion device to be installed, a U-49 undulator, has been assembled and magnetically measured. The r.m.s. phase error is 2°. An endpole configuration using coils with less than 64 amp-turns makes the angular kick smaller than ±3 μrad over a gap range 15–50 mm.

**Keywords: insertion devices; phase errors.**

## 1. Overview

The synchrotron radiation light source BESSY II has an electron energy of 1.7 GeV and a horizontal emittance of $\epsilon_x = 6 \times 10^{-9}\pi$ mrad. The 16 straight sections have alternating horizontal $\beta$-functions of ~1 m for superconducting wavelength shifters and short undulators (3.4 m), and of ~16 m for undulators and wigglers up to 4.2 m long.

In this article we focus on the permanent-magnet devices. They have been designed, constructed and assembled at BESSY. The basic parameters are summarized in Table 1.

The long-period devices U/W-125 will be supplied with die-pressed aluminium vacuum chambers which allow for a minimum magnetic gap of 20 mm. The U-49 undulators are optimized for the same magnetic gap. Later, a so-called small-aperture chamber (11 mm vacuum gap) will be installed which allows a minimum magnetic gap of 15 mm and hence an extension of the energy range to longer wavelengths. The circularly polarizing undulators UE-56 have to be equipped with the small-aperture chamber in order to provide purely circularly polarized light below 100 eV. The U-41 undulator is designed for microscopy applications. Even with the large-aperture chamber, the C, N and O *K*-edges are covered by the first harmonic. However, the small-aperture chamber is necessary for providing an overlap of the first and third harmonic.

## 2. Mechanical performance

Support and drive systems for the various permanent-magnet insertion devices have a modular design. Base and C-structures are made from cast iron. The beams supporting the magnetic structures and the fixture for poles and magnets are made from aluminium. The magnetic structure of the long insertion devices (4.2 m) is divided longitudinally into two parts for mechanical reasons. The gap-change drive uses servomotors with the feedback signal derived from linear encoders measuring the gap. The drive system for the long devices has been characterized in detail, simulating magnetic forces up to 15 kN per axis by a stack of springs (Bahrdt *et al.*, 1995, 1996; Bäcker *et al.*, 1995). The servomotor system compensates within less than ±1 μm for the mechanical backlash of about 30 μm.

With the magnets installed, the encoder is mounted about 300 mm off-axis, violating Abbe's comparator principle: a beam roll during gap drive leads to a measurement error. Therefore, a stiff coupling to linear bearings defining the line of motion is essential. Monitoring the magnetic field during gap change showed hysteresis effects due to a residual bending of the joints between the beams and the linear bearings caused by the friction in the latter ones of up to 8 μm (see Fig. 1). Using a second linear encoder at the far side of the beam reduced the error to below 3 μm.

We studied the dynamic performance of our drive system for the case of a linear energy *versus* time relation. The corresponding velocity profile varies between 1 and 1.6 mm $s^{-1}$. This profile has been downloaded to the servomotor controller. The deviation between the ideal gap and the measured gap is less than

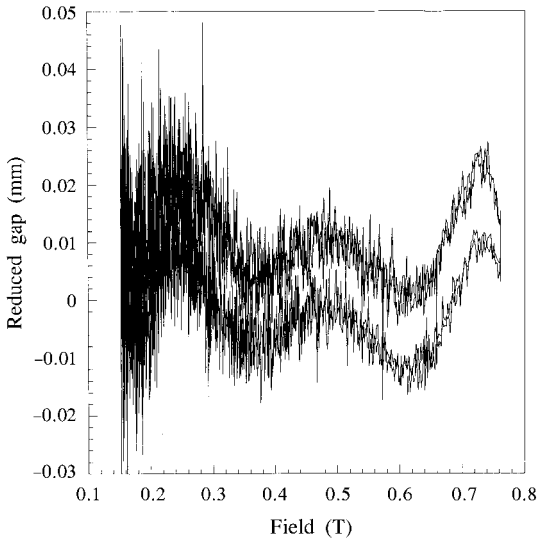


**Figure 1**
Reduced-gap reading *versus* measured magnetic field for several gap opening and closing cycles. The reduced gap has been derived from the measured gap *via* subtraction of an eighth-order polynomial.

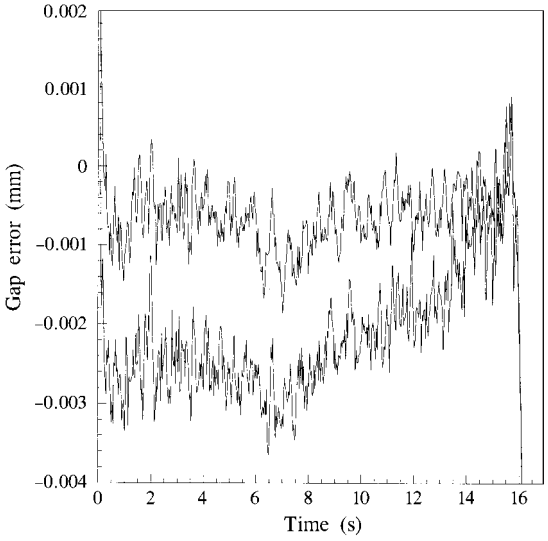


**Figure 2**
Gap error of two axes during a non-uniform gap drive. The gap speed varies between 1.0 and 1.6 mm $s^{-1}$.

**Table 1**
Insertion devices for BESSY II.

| Name | U-125 | W-125† | U-49 | U-41 | UE-56 |
|---|---|---|---|---|---|
| Number of insertion devices | 2 | | 2 | 1 | 2 |
| $\lambda_0$ (mm) | 125 | 125 | 49.4 | 41 | 56 |
| Periods | 32 | 32 | 84 | 81 | 2 × 31 |
| $L$ (m) | 4.0 | 4.0 | 4.2 | 3.35 | 2 × 1.74 |
| Minimum magnetic gap (mm) | 20 | 20 | 15 | 15 | 16 |
| Minimum vacuum gap (mm) | 16 | 16 | 11 | 11 | 11 |
| Design | Hybrid Straight poles | Hybrid Straight poles | Hybrid Wedged poles | Hybrid Wedged poles | PPM‡ |
| $B_0$ (T) | 0.55 | 1.15 | 0.82 | 0.67 | 0.63 |

† U-125 device operating in the wiggler mode. ‡ Pure permanent-magnet device of the Sasaki type (Sasaki *et al.*, 1993).

3 μm for both axes (Fig. 2), corresponding to a photon energy deviation of $\Delta E/E = 2 \times 10^{-4}$, which is less than one-tenth of the width of the fifth harmonic for U-49.

### 3. Magnetic measurements of the U-49 undulator

The periodic part of the U-49 undulator consists of 84 periods, each 49.4 mm long. There are 336 wedged-shaped poles made from permendur and three times as many wedged-shaped permanent magnets made of NdFeB. The dipole moments of the magnets, as measured in an automized Helmholtz-coil set-up, are used to assign positions to individual magnets using the technique of simulated annealing. The assembly of the magnetic structure is controlled at intermediate steps using a three-dimensional coordinate-measuring machine and a laser interferometer. All pole faces of one I-beam are found to be in a plane within ±20 μm. No shimming based on magnetic measurements has been performed besides centring some ten magnets within the adjacent poles.

The endpole configuration consists of a pole piece sandwiched between two permanent magnets (similar to the ESRF design; Chavanne *et al.*, 1995). Using three-dimensional magnetostatic field calculations, a geometry is chosen that minimizes the kick and the displacement within the end section over the operating range of the gap between 15 and 50 mm. Without any further experimental improvements of the geometry, a coil of less than 64 amp-turns was sufficient to compensate for the residual kick.

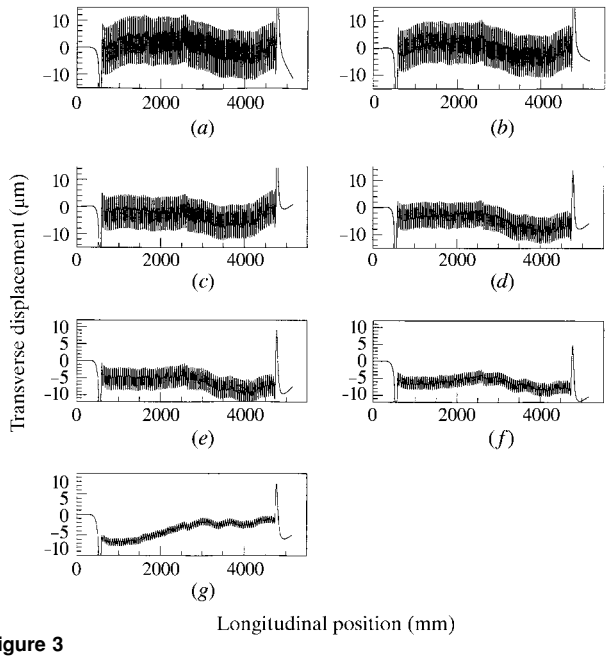


**Figure 3**
Trajectories of the U-49 undulator at various gaps. The upstream endpole is compensated over the entire gap range with compensation currents of $|I| \leq 64$ amp-turns. The coil of the downstream endpole is not powered. Gap = (*a*) 15, (*b*) 17, (*c*) 20, (*d*) 24, (*e*) 30, (*f*) 38 and (*g*) 50 mm.

Here we concentrate on magnetic field measurements using a Hall probe at our 5.5 m measuring bench. This apparatus allows the Hall probe to be moved under computer control along three orthogonal axes, $x$, $y$, $z$, and to be rotated (around the transverse axis $z$) by the angle $\theta$. Positions are determined using a laser interferometer for the long axis and linear and rotary encoders for the short axis (travel 100 mm) and the rotation, respectively.

On-axis measurements of the vertical magnetic field component have been made for various gap values. The second field integral, being proportional to the electron trajectory, is shown in Fig. 3. The phase errors are calculated according to

$$\Delta\Phi = [2\pi/\beta\lambda(B\rho)^2] \int_0^z \left[ \int_0^{z'} B_y^{\text{fit}}\, \mathrm{d}z'' \times \int_0^{z'} B_y^{\text{res}}\, \mathrm{d}z'' + \left( \int_0^{z'} B_y^{\text{res}}\, \mathrm{d}z'' \right)^2 /2 \right] \mathrm{d}z'. \quad (1)$$

$B^{\text{fit}}$ is the fit to the data using a sum of five sinusoidal components with odd multiples of the basic periodicity. $B^{\text{res}}$ is the corresponding residual. This expression is obtained from the integral over the square of the slope of the electron trajectory omitting the ideal field contribution. After a straight-line subtraction, which corresponds to a retuning of the photon energy, the r.m.s. values of the optical phase error for gaps of 15, 17, 20, 24, 30, 38 and 50 mm are 2.0, 1.9, 1.9, 1.7, 1.5, 1.1 and 0.5°, respectively. Thus, magnetic field errors will only insignificantly reduce the optical performance up to the fifth harmonic.

### References

Bäcker, H., Bahrdt, J., Gaupp, A., Gottschlich, S., Horn, R., Ingold, G. & Meyer, G. (1995). BESSY Annual Report, pp. 539–541. BESSY, Berlin, Germany.

Bahrdt, J., Blümer, K., Gaupp, A., Ingold, G., Noll, T., Paziranebeh, R., Scheer, M. & Stahr, F. (1995). BESSY Annual Report, pp. 542–543. BESSY, Berlin, Germany.

Bahrdt, J., Gaupp, A., Ingold, G. & Scheer, M. (1996). *Proc. EPAC96*, Sitges, Barcelona, Vol. 3, pp. 2535–2537. Bristol: Institute of Physics.

Chavanne, J., Elleaume, P. & Van Vaerenbergh, P. (1995). *Proc. PAC95*, Dallas, Vol. 2, pp. 1319–1321. Piscataway, NJ: IEEE.

Sasaki, S., Kakuno, K., Takada, T., Shimada, T., Yanagida, K. & Miyahara, Y. (1993). *Nucl. Instrum. Methods*, A**331**, 763–767.